

Measurement of Barriers for Alkene Dissociation and for Inversion at Zirconium in a d^0 Zirconium–Alkyl–Alkene Complex

Charles P. Casey* and Donald W. Carpenetti II

Department of Chemistry, University of Wisconsin, Madison, Wisconsin 53706

Received November 8, 1999

The β -allyl zirconacyclobutane complex $\text{Cp}^*_2\text{Zr}[\text{CH}_2\text{CH}(\text{CH}_2\text{CH}=\text{CH}_2)\text{CH}_2]$ (**7**) reacted rapidly with $\text{B}(\text{C}_6\text{F}_5)_3$ in CD_2Cl_2 at -78°C to form the zwitterionic d^0 zirconium(IV) chelate complex $\text{Cp}^*_2\text{Zr}[\eta^1, \eta^2\text{-CH}_2\text{CH}[\text{CH}_2\text{B}(\text{C}_6\text{F}_5)_3]\text{CH}_2\text{CH}=\text{CH}_2]$ (**2a** and **2b**). Low-temperature ^1H , ^{13}C , TOCSY1D, and NOESY1D NMR spectroscopy of **2** established the bonding of the tethered alkene to the d^0 metal center. A dynamic NMR study of the interconversion of **2a** and **2b** allowed measurement of the alkene dissociation energy ($\Delta G^\ddagger = 10.5$ (**2a** to **2b**) and 10.3 (**2b** to **2a**) kcal mol^{-1}), but the complex decomposed before the barrier for site epimerization at the zirconium center could be determined. Reaction of **7** with $[(\text{C}_6\text{H}_5)_2(\text{CH}_3)\text{NH}][\text{B}(\text{C}_6\text{F}_5)_4]$ led to the formation of two isomeric d^0 zirconium(IV)–alkyl–alkene chelates $\text{Cp}^*_2\text{Zr}[\eta^1, \eta^2\text{-CH}_2\text{CH}(\text{CH}_3)\text{CH}_2\text{CH}=\text{CH}_2][\text{B}(\text{C}_6\text{F}_5)_4]$ (**8a** and **8b**). This more thermally stable zirconium–alkyl–alkene complex allowed the measurement of barriers associated with decomplexation of the alkene ($\Delta G^\ddagger = 10.7$ and 11.1 kcal mol^{-1}) and site epimerization at the zirconium center ($\Delta G^\ddagger = 14.4$ kcal mol^{-1}) by line shape analysis of variable-temperature ^1H and ^{13}C NMR spectra.

Introduction

d^0 metal–alkyl–alkene complexes have been proposed as crucial but unobserved intermediates¹ in metallocene-catalyzed alkene polymerizations.² These intermediates have eluded observation presumably because of their high kinetic reactivity and their low thermodynamic stability due to the absence of d to π^* back-bonding. Recently, we reported the first d^0 metal–alkyl–alkene complex, $\text{Cp}^*_2\text{Y}(\eta^1, \eta^2\text{-CH}_2\text{CH}_2\text{C}(\text{CH}_3)_2\text{CH}=\text{CH}_2)$ (**1**),³ which is stabilized by chelation. Subsequently, we reported detailed analyses of the kinetics and thermodynamics of d^0 yttrium–alkyl–alkene complexes.⁴ We have also recently published a preliminary report on a d^0 zirconium–alkyl–alkene complex, the

zwitterionic complex $\text{Cp}^*_2\text{Zr}^+[\eta^1, \eta^2\text{-CH}_2\text{CH}\{\text{CH}_2\text{B}^-(\text{C}_6\text{F}_5)_3\}\text{CH}_2\text{CH}=\text{CH}_2]$ (**2**).⁵ Other reported examples of d^0 zirconium–alkene complexes include Jordan's alkoxy–alkene complex $[\text{Cp}_2\text{Zr}(\eta^1, \eta^2\text{-OCMe}_2\text{CH}_2\text{CH}_2\text{CH}=\text{CH}_2)]\text{-}[\text{MeB}(\text{C}_6\text{F}_5)_3]$ (**3**),⁶ Royo's $[(\text{Cp})(\eta^5, \eta^2\text{-C}_5\text{H}_4\text{SiMe}_2\text{CH}_2\text{-CH}=\text{CH}_2)\text{Zr}(\text{CH}_2\text{C}_6\text{H}_5)][\text{B}(\text{C}_6\text{F}_5)_4]$ (**4**),⁷ and Erker's $(\text{MeCp})_2\text{Zr}^+\text{CH}_2\text{CH}(\text{CH}_3)\text{CH}_2\text{CH}=\text{CHCH}_2\text{B}^-(\text{C}_6\text{F}_5)_3$ (**5**) and related complexes (Scheme 1).⁸ Our studies have shown that complexation of an alkene to a d^0 yttrium or zirconium center polarizes the π -bond, that decomplexation is fast at low temperature, and that there is a significant barrier to inversion at pyramidal Cp^*_2YR centers.⁹

The stereochemistry of metallocene-catalyzed propylene polymerization is controlled by the microstructure of the catalysts and in some cases by the ability of the zirconium alkyl to undergo inversion of configuration at the metal center. Highly isotactic polypropylene can be formed using C_2 -symmetric metallocene catalysts,¹⁰ as the tacticity is not affected by the rate of inversion at the metal center since the same enantioface of propene coordinates selectively to either of the C_2 -related sites. Highly syndiotactic polypropylene can be

(1) (a) Cossee, P. *J. Catal.* **1964**, *3*, 80. (b) Arlman, E. J.; Cossee, P. *J. Catal.* **1964**, *3*, 99. (c) Brookhart, M.; Green, M. L. H.; Wong, L.-L. *Prog. Inorg. Chem.* **1988**, *36*, 1. (d) Brookhart, M.; Volpe, A. F.; Lincoln, D. M.; Horváth, I. T.; Millar, J. M. *J. Am. Chem. Soc.* **1990**, *112*, 5634. (e) Brookhart, M.; Green, M. L. H. *J. Organomet. Chem.* **1983**, *250*, 395. (f) Dawoodi, Z.; Green, M. L. H.; Mtetwa, V. S. B.; Prout, K. J. *Chem. Soc., Chem. Commun.* **1982**, 1410. (g) Ivin, K. J.; Rooney, J. J.; Stewart, C. D.; Green, M. L. H.; Mahtab, R. *J. Chem. Soc., Chem. Commun.* **1978**, 604.

(2) For reviews of metallocene-catalyzed alkene polymerization, see: (a) Jordan, R. F. *Adv. Organomet. Chem.* **1991**, *32*, 325. (b) Brintzinger, H. H.; Fisher, D.; Mühlaupt, R.; Rieger, B.; Waymouth, R. M. *Angew. Chem., Int. Ed. Engl.* **1995**, *34*, 1143. (c) Marks, T. J. *Acc. Chem. Res.* **1992**, *25*, 57. (d) Bochmann, M. *J. Chem. Soc., Dalton Trans.* **1996**, 255. (e) Alt, H. G.; Koppl, A. *Chem. Rev.* **2000**, *100*, 1205. (f) Resconi, L.; Cavallo, L.; Fait, A.; Pietmontesi, F. *Chem. Rev.* **2000**, *100*, 1253. (g) Chen, E. Y.-X.; Marks, T. J. *Chem. Rev.* **2000**, *100*, 1391. (h) Rappe, A. K.; Skiff, W. M.; Casewitt, C. J. *Chem. Rev.* **2000**, *100*, 1435.

(3) Casey, C. P.; Hallenbeck, S. L.; Pollock, D. W.; Landis, C. R. *J. Am. Chem. Soc.* **1995**, *117*, 9770.

(4) (a) Casey, C. P.; Hallenbeck, S. L.; Wright, J. M.; Landis, C. R. *J. Am. Chem. Soc.* **1997**, *119*, 9680. (b) Casey, C. P.; Fisher, J. J. *Inorg. Chim. Acta* **1998**, *270*, 5. (c) Casey, C. P.; Fagan, M. A.; Hallenbeck, S. L. *Organometallics* **1998**, *17*, 287. (d) Casey, C. P.; Fisher, J. J.; Fagan, M. A. *J. Am. Chem. Soc.* **2000**, *122*, 4320.

(5) For a preliminary communication, see: Casey, C. P.; Carpenetti, D. W., II; Sakurai, H. *J. Am. Chem. Soc.* **1999**, *121*, 9483.

(6) Wu, Z.; Jordan, R. F.; Petersen, J. L. *J. Am. Chem. Soc.* **1995**, *117*, 5867.

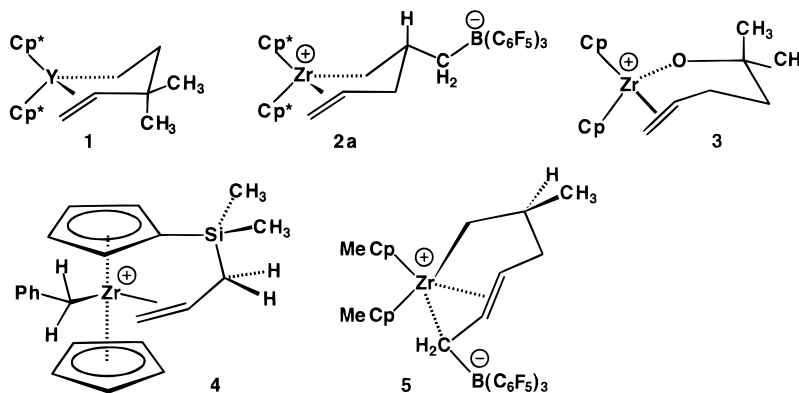
(7) Galakhov, M. V.; Heinz, G.; Royo, P. *Chem. Commun.* **1998**, 17.

(8) Temme, B.; Karl, J.; Erker, G. *Chem. Eur. J.* **1996**, *2*, 919.

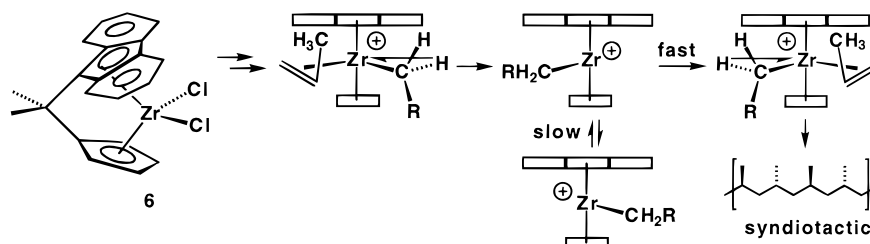
(9) Inversion at the metal center has also been called site epimerization and back slipping.

(10) (a) Coughlin, E. B.; Bercaw, J. E. *J. Am. Chem. Soc.* **1996**, *118*, 12021. (b) Herzog, T. A.; Zubris, D. L.; Bercaw, J. E. *J. Am. Chem. Soc.* **1996**, *118*, 11988. (c) Cavallo, L.; Guerra, G.; Vacatello, M.; Corrandini, P. *Macromolecules* **1991**, *24*, 1784. (d) Busico, V.; Corrandini, P.; De Biasio, R.; Landriani, L.; Segre, A. L. *Macromolecules* **1994**, *27*, 4521.

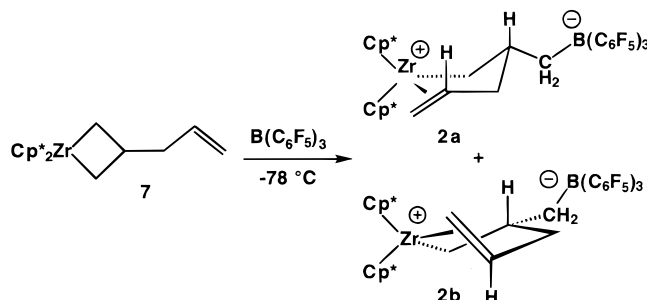
Scheme 1



Scheme 2



Scheme 3



formed using C_5 -symmetric metallocenes, such as Ewen's (**6**).¹¹ In this case, the stereochemistry of the polymer depends on the relative rates of insertion of the next monomer and inversion at the metal center (Scheme 2). One of our main goals in studying models of intermediates related to these polymerization catalysts is to measure the barrier associated with this process of inversion at the zirconium center.

Our early attempts to produce a zirconium–alkyl–alkene complex focused on protonation routes employing ammonium cations, noncoordinating anions, and Stryker's β -allyl zirconacyclobutane, $\text{Cp}^*_2\text{Zr}[\text{CH}_2\text{CH}(\text{CH}_2\text{CH}=\text{CH}_2)\text{CH}_2]$ (**7**).¹² An early protonation route employing $[\text{C}_6\text{H}_5(\text{CH}_3)_2\text{NH}][\text{B}(\text{C}_6\text{F}_5)_4]$ failed to give the desired alkene complex. Instead, coordination of the conjugate base to zirconium occurred to give $[\text{Cp}^*_2\text{Zr}\{\text{N}(\text{CH}_3)_2\text{C}_6\text{H}_5\}\text{CH}_2\text{CH}(\text{CH}_3)\text{CH}_2\text{CH}=\text{CH}_2][\text{B}(\text{C}_6\text{F}_5)_4]$ in quantitative yield. Attempts to generate a zwitterionic zirconium–alkyl–alkene complex using the alkyl group abstractor $\text{B}(\text{C}_6\text{F}_5)_3$ were successful and allowed the observation of two isomers of $\text{Cp}^*_2\text{Zr}[\eta^1, \eta^2\text{-CH}_2\text{CH}[\text{CH}_2\text{B}(\text{C}_6\text{F}_5)_3]\text{-CH}_2\text{CH}=\text{CH}_2]$ (**2a** and **2b**). We were able to measure the barrier for alkene decomplexation, but the thermal instability of **2** prevented measurement of the barrier to inversion at zirconium, an important factor in the production of syndiotactic polypropylene.

In the work reported here, we have protonated Stryker's β -allyl zirconacyclobutane **7**¹⁴ with $[(\text{C}_6\text{H}_5)_2\text{CH}_3\text{NH}][\text{B}(\text{C}_6\text{F}_5)_4]$, which generates a more sterically inaccessible and much less Lewis basic amine conjugate base. This procedure produced two isomers of the

cationic zirconium–alkyl–alkene complex $\text{Cp}^*_2\text{Zr}[\eta^1, \eta^2\text{-CH}_2\text{CH}(\text{CH}_3)\text{CH}_2\text{CH}=\text{CH}_2][\text{B}(\text{C}_6\text{F}_5)_4]$ (**8a** and **8b**). These isomers proved to be more thermally stable than the corresponding zwitterions **2a** and **2b** and allowed the measurement of both the barrier decomplexation as well as the additional barrier corresponding to inversion at the zirconium center.⁹

Results

Alkyl Group Abstraction Route to Zirconium–Alkyl–Alkene Complexes.⁵ The reaction of Stryker's β -allyl zirconacyclobutane complex **7**¹² with $\text{B}(\text{C}_6\text{F}_5)_3$ ¹³ generated the first example of a stable zwitterionic d^0 zirconium–alkyl–alkene complex with an all-carbon chelate backbone (Scheme 3). Reaction of **7** with $\text{B}(\text{C}_6\text{F}_5)_3$ in CD_2Cl_2 at -78°C led to the formation of a bright orange solution containing a 1.8:1 mixture of two diastereomers of the zwitterionic d^0 zirconium(IV)–alkyl–alkene chelate complex $\text{Cp}^*_2\text{ZrCH}_2\text{CH}[\text{CH}_2\text{B}(\text{C}_6\text{F}_5)_3]\text{CH}_2\text{CH}=\text{CH}_2$ (**2a** and **2b**).

There are two diastereomers of **2** due to the presence of two stereogenic centers, the β -carbon of the chelate chain and the *re* or *si* face of the alkene. The two diastereomers were identified by ^1H and ^{13}C NMR spectroscopy at -82°C . The major diastereomer is assumed to have the alkyl substituent in the pseu-

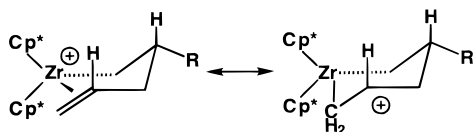
(11) (a) Ewen, J. A.; Jones, R. L.; Razavi, A.; Ferrara, J. D. *J. Am. Chem. Soc.* **1988**, *110*, 6255. (b) Ewen, J. A. *Makromol. Chem., Macromol. Symp.* **1995**, *89*, 181.

(12) Tjaden, E. B.; Stryker, J. M. *J. Am. Chem. Soc.* **1993**, *115*, 2083.

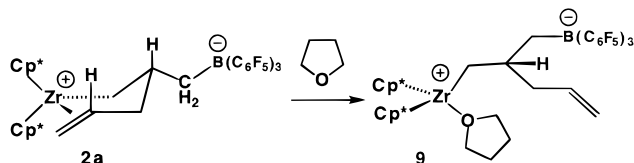
(13) Massey, A. G.; Park, A. J. *J. Organomet. Chem.* **1964**, *2*, 245.

(14) These compounds were synthesized by a procedure similar to that of: Tjaden, E. B.; Swenson, D. C.; Jordan, R. F.; Petersen, J. L. *Organometallics* **1995**, *14*, 371.

Scheme 4



Scheme 5



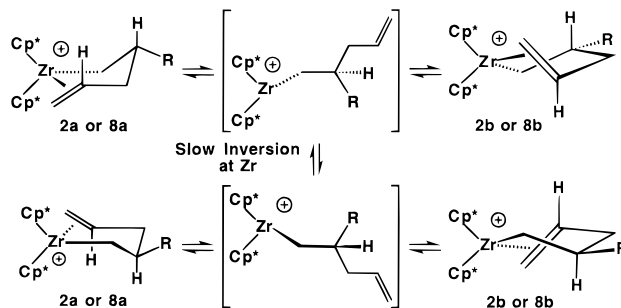
doequatorial position. The most striking feature in the ^1H NMR spectrum of these complexes is the high-frequency chemical shifts of the secondary vinyl protons of the coordinated alkene compared to those of **7**. Upon coordination, the secondary vinyl proton experiences a large shift to higher frequency from δ 6.29 in **7** to 7.92 in the major isomer **2a** (+1.63 ppm) and to δ 7.54 ppm in the minor isomer **2b** (+1.25 ppm). Similar shifts to higher frequency upon alkene coordination to a d^0 metal are seen for **1** (+1.04 ppm), **3** (+1.64), and **4** (+1.58). This shift to higher frequency can be attributed to a resonance contributor that allows delocalization of positive charge from zirconium to the internal vinyl carbon (Scheme 4). Greatly increased separation of the terminal vinyl proton resonances also support alkene coordination. **7** shows these resonances at δ 5.25 and 5.14 ($\Delta\delta = 0.09$ ppm). For major chelate isomer **2a**, these resonances are observed at δ 5.85 and 2.44 ($\Delta\delta = 3.41$ ppm); for **2b**, they are observed at δ 5.73 and 2.27 ($\Delta\delta = 3.46$). The coupling constants between the vinyl protons of **2a** and **2b** are similar to those of free alkenes.

In the ^{13}C NMR spectrum of **2a** and **2b**, the ZrCH_2 resonances at δ 75.7 (**2a**) and 73.2 (**2b**) confirm the presence of an alkyl group bound to a zirconium cation. The shifts to higher frequency of the internal vinyl carbon resonances of **2a** ($\Delta\delta = +22.4$) and **2b** ($\Delta\delta = +25.5$) relative to those of **7** provide further evidence for alkene coordination and polarization of the alkene double bond.

Addition of THF to the solution of **2a** and **2b** at -78°C in CD_2Cl_2 led to the immediate displacement of the coordinated alkene and formation of a bright yellow solution of a single 1:1 THF adduct, $\text{Cp}^*_2\text{Zr}(\text{THF})\text{CH}_2\text{CH}[\text{CH}_2\text{B}(\text{C}_6\text{F}_5)_3]\text{CH}_2\text{CH}=\text{CH}_2$ (**9**) (Scheme 5). The ^1H NMR chemical shifts of the vinyl hydrogens (δ 5.73, 4.92, 4.89) and the ^{13}C NMR chemical shifts of the vinyl carbons (δ 114.9 and 138.1) of **9** are very similar to those of **7** and very different from those of **2a** and **2b**, providing evidence that coordination of THF displaces the alkene from zirconium.

Further evidence for coordination of the alkene was obtained from 1D NOE difference spectra of the major isomer **2a**. Due to the presence of other resonances in the same region of the spectrum as the resonances of the Cp^* protons, the only unambiguous NOE experiments involved the unfavorable NOE transfer from the vinyl protons of the chelate to the Cp^* methyl protons. Approximately 1% positive enhancements were observed between one terminal vinyl hydrogen and one Cp^* ligand ($H_E\text{--Cp}^*$ δ 1.96), between the other terminal

Scheme 6



vinyl hydrogen and the other Cp^* ligand ($H_Z\text{--Cp}^*$ δ 1.98), and between the secondary vinyl proton and the Cp^* at δ 1.98. In contrast, for the nonchelated THF adduct **9**, no NOE enhancements of Cp^* peaks were detected upon irradiation of the vinyl protons.

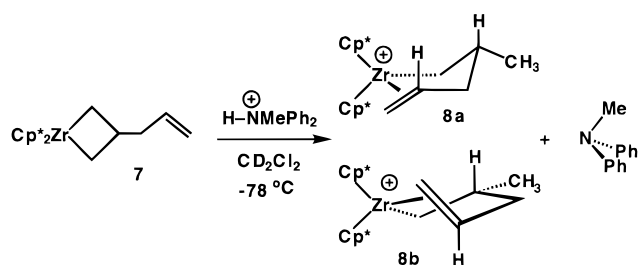
Upon slow warming of the solution to -42°C , **2a** and **2b** interconvert rapidly and the individual resonances of **2a** and **2b** coalesce into one set of weighted average resonances (Scheme 6). The four original Cp^* resonances converge to two distinct resonances at δ 2.03 and 2.01; each new resonance corresponds to the weighted average of two of the original four Cp^* resonances. The interconversion of **2a** and **2b** is consistent with a dynamic process that involves decomplexation of the bound face of the alkene and recoordination to the other enantioface. This process renders the secondary vinyl proton resonances of **2a** and **2b** equivalent. All temperature-dependent changes are reversible up to -35°C , but significant decomposition occurs at higher temperatures. Line shape analysis of the coalescence of the secondary vinyl hydrogen resonances gave $\Delta G^\ddagger = 10.5$ kcal mol $^{-1}$ for **2a** to **2b** and $\Delta G^\ddagger = 10.3$ kcal mol $^{-1}$ for **2b** to **2a**.

The barrier to alkene dissociation from zirconium in **2** is significantly higher than from similar neutral yttrium chelates ($\Delta G^\ddagger_{\text{diss}} = 7.5$ kcal mol $^{-1}$ for $\text{Cp}^*_2\text{YCH}_2\text{CH}_2\text{CH}=\text{CH}_2$), presumably due to stronger alkene binding to a cationic zirconium center than to a neutral yttrium center. The alkene dissociation barrier of **2** is similar to that of other cationic zirconium chelates ($\Delta G^\ddagger_{\text{diss}} = 10.7$ kcal mol $^{-1}$ for Jordan's compound **3**).⁶ The combined barrier for alkene dissociation and zirconium inversion from Royo's compound **4** is 11.7 kcal mol $^{-1}$.⁷

Two distinct Cp^* resonances for **2** are observed up to temperatures where decomposition starts to occur; this is consistent with slow inversion at zirconium. Line shape analysis of the Cp^* resonances observed before decomposition leads to an estimate that $\Delta G^\ddagger_{\text{invers}} \approx 15$ kcal mol $^{-1}$ for **2** in CD_2Cl_2 .

Protonation Route to Zirconium-Alkyl-Alkene Complexes. In an initial attempt to generate a cationic d^0 zirconium-alkyl-alkene complex by protonation, we treated Stryker's β -allyl zirconacyclobutane **7**¹² with $[\text{C}_6\text{H}_5(\text{CH}_3)_2\text{NH}][\text{B}(\text{C}_6\text{F}_5)_4]$ ¹⁴ at -78°C in CD_2Cl_2 . However, instead of intramolecular alkene coordination, the amine conjugate base *N,N*-dimethylaniline coordinated to the electrophilic zirconium center to give $\{\text{Cp}^*_2\text{Zr}[\text{N}(\text{CH}_3)_2\text{C}_6\text{H}_5][\eta^1\text{--CH}_2\text{CH}(\text{CH}_3)\text{CH}_2\text{CH}=\text{CH}_2]\}[\text{B}(\text{C}_6\text{F}_5)_4]$ (**10**). Evidence for amine coordination came from ^1H NMR chemical shifts; the *N*-methyl groups of amine complex **10** appeared at δ 3.65 compared with δ 3.19

Scheme 7



for the free amine. Similar amine complexes were formed upon protonation by analogous tributylammonium and (diisopropyl)ethylammonium salts.

In an effort to avoid amine complexation, we employed the conjugate acid of a less basic and more sterically crowded amine. Reaction of [(C₆H₅)₂(CH₃)NH][B(C₆F₅)₄]¹⁴ with **7** led to the formation of a yellow-brown solution. ¹H and ¹³C NMR spectra at -78 °C provided evidence for a 2.2:1 mixture of two isomers of Cp*₂Zr[η¹,η²-CH₂-CH(CH₃)CH₂CH=CH₂][B(C₆F₅)₄] (**8a** and **8b**) and free diphenyl(methyl)amine (**11**) (Scheme 7). The ratio of diastereomers of **8** was similar to the 1.8:1 ratio seen for the zwitterionic analogue **2**. Perturbation of the vinyl hydrogen chemical shifts compared to those of **7** provided evidence for alkene complexation. The secondary vinyl hydrogen of **8a** appears at δ 7.89, shifted 1.60 ppm to higher frequency than in **7** and that of **8b** is shifted 1.20 ppm to δ 7.49. In contrast with the small differences between the chemical shifts of the terminal vinyl hydrogens of the uncomplexed alkene of **7** (δ 5.25, 5.14, Δδ = 0.09 ppm), large chemical shift differences are seen for the complexed alkene in both **8a** [δ 5.43 (*J*_{trans} = 17.1 Hz), 2.44 (*J*_{cis} = 10.1 Hz), Δδ = 2.99 ppm] and **8b** [δ 5.71 (*J*_{trans} = 17.8 Hz), 2.18 (*J*_{cis} = 12.5 Hz), Δδ = 3.53 ppm]. At low temperatures, four Cp* resonances are observed, two for **8a** and two for **8b**.

Further evidence for alkene coordination in **8a** and **8b** comes from ¹³C NMR spectroscopy. The internal vinyl carbon resonance of **8a** at δ 163.0 was shifted 21.8 ppm to higher frequency than in **7** and that of **8b** at δ 166.1 was shifted 24.9 ppm to higher frequency. As in the case of the zwitterionic chelates **2a** and **2b**, the shifts of the terminal vinyl carbons of **8a** and **8b** are similar to those of the uncomplexed alkene of **7**. Characteristic high-frequency resonances at δ 75.1 **8a** and 72.6 **8b** provided evidence for Zr⁺CH₂ groups.

Displacement of the coordinated alkene was observed upon addition of THF to a CD₂Cl₂ solution of **8a** and **8b** at -78 °C, yielding a yellow solution of the single THF adduct Cp*₂Zr(THF)[CH₂CH(CH₃)CH₂CH=CH₂]⁺[B(C₆F₅)₄]⁻ (**12**). The ¹H and ¹³C NMR chemical shifts of the vinyl group of **12** are consistent with a noncoordinated alkene.

Coordination of the alkene to the zirconium center is further supported by 1D NOE spectroscopy of **8a**. The Cp* resonance at δ 1.98 received a 3.0 ± 0.5% NOE enhancement when either the secondary vinyl hydrogen or the terminal vinyl hydrogen cis to it (δ 2.44) was irradiated. The Cp* resonance at δ 1.96 received a 2.8 ± 0.5% NOE enhancement when the other terminal vinyl hydrogen at δ 5.43 was irradiated. In contrast, no

NOE was observed between the Cp* and vinyl resonances of the THF complex **12**.

Upon slowly raising the temperature from -78 to -38 °C, the resonances of **8a** and **8b** broadened and coalesced to give one set of weighted average resonances (Scheme 6). The four original Cp* resonances converge to two distinct resonances at δ 2.02 and 2.00; each new resonance corresponds to the weighted average of two of the original four Cp* resonances. The interconversion of **8a** and **8b** occurs by alkene dissociation and recoordination of the opposite alkene enantioface.

The internal vinyl proton resonance of **8b** was partially obscured by the aryl resonances of diphenyl(methyl)amine, making simulation of this coalescence impossible. Therefore, the rate of interconversion of **8a** and **8b** was measured by following the coalescence of the resonances corresponding to the tertiary proton on the β-carbon of the alkyl chain. The baseline was flat in the area of these resonances, and line shapes were accurately simulated using the DNMR program.¹⁵ Coalescence was observed at -38 °C, and the resonances became relatively sharp at -28 °C. Line shape analysis gave Δ*G*[‡] = 10.7 ± 0.2 kcal mol⁻¹ for **8b** to **8a** and Δ*G*[‡] = 11.1 ± 0.2 kcal mol⁻¹ for **8a** to **8b**.¹⁶ These barriers are similar to those observed for zirconium alkene complexes **2a** and **2b** (Δ*G*[‡] = 10.3 and 10.5 kcal mol⁻¹)⁵ and **3** (Δ*G*[‡] = 10.7 kcal mol⁻¹)⁶ and higher than those observed for the related neutral yttrium compound **1** (Δ*G*[‡] = 8.2 kcal mol⁻¹).^{4d}

Upon further warming, the two Cp* resonances of the rapidly equilibrating mixture of **8a** and **8b** broadened and coalesced into a single resonance at 2 °C. None of the other resonances in the spectrum were affected. This coalescence is consistent with dissociation of alkene from zirconium, inversion at zirconium, rotation about the Zr-C bond, and recoordination of the alkene (Scheme 8). All temperature-dependent changes are reversible, but decomposition begins to occur at -5 °C and is rapid at +5 °C.¹⁷ Line shape analysis of this process yielded Δ*G*[‡] = 14.4 ± 0.9 kcal mol⁻¹ (Δ*H*[‡] = 14.0 ± 0.7 kcal mol⁻¹; Δ*S*[‡] = -1 ± 2 eu). Previously, we observed a 9.6 kcal mol⁻¹ barrier for alkene dissociation and inversion at yttrium for Cp*₂YCH₂CH₂CH(CH₃)CH=CH₂.^{4c} Marks found that for [(1,2-Me₂C₅H₃)₂ZrCH₃][CH₃B(C₆F₅)₃] the barrier for ion pair dissociation and inversion at zirconium was strongly solvent dependent and was 11 kcal mol⁻¹ in C₆D₅Cl.¹⁸

The possible involvement of associative processes in alkene decomplexation and inversion was investigated. The possibility that (C₆H₅)₂CH₃N (**11**) or borate ion pairs might displace the alkene was investigated by increasing the concentration of both species. Changing the concentration of the solution containing zirconium-alkyl-alkene complexes **8a**, **8b**, and amine **11** did not change the barriers for alkene decomplexation or inversion measured by dynamic NMR spectroscopy. This finding rules out any contribution from associative pathways involving interaction between chelate complexes or interaction with free amine. Added [Ph-

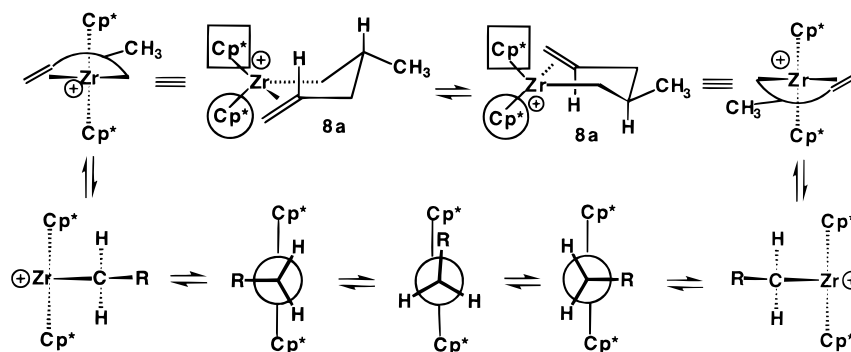
(16) Δ*H*[‡] = 14.0 ± 0.2 kcal mol⁻¹ and Δ*S*[‡] = 14 ± 1 eu for **8b** to **8a**; Δ*H*[‡] = 14.0 ± 0.2 kcal mol⁻¹ and Δ*S*[‡] = 12 ± 1 eu for **8a** to **8b**.

(17) The half-life of **8** was 60 min at -5 °C, 17 min at 5 °C, and 5.4 min at 15 °C. This instability prevented us from obtaining ¹³C NMR spectra at these temperatures.

(18) Deck, P. A.; Marks, T. J. *J. Am. Chem. Soc.* **1995**, *117*, 6128.

(15) Reich, H. J. *J. Chem. Educ.* **1995**, *72*, 1086.

Scheme 8



(CH₃)₃N][B(C₆F₅)₄] was also found to have no effect on the barriers for alkene decomplexation and inversion. When solvent was changed from CD₂Cl₂ to C₆D₅Cl, the barriers were the same, implying that solvent is not involved in either process.¹⁹

Having ruled out the involvement of B(C₆F₅)₄[−] in the dynamic processes involving zirconium–alkyl–alkene chelates, we turned our attention to the CH₃B(C₆F₅)₃ anion. This anion is of considerable interest, because addition of B(C₆F₅)₃ to methyl–zirconocenes usually results in the formation of Zr–CH₃–B(C₆F₅)₃-bridged species, even in the presence of bulky Cp* ligands.²⁰ To determine whether the CH₃B(C₆F₅)₃[−] would displace the chelated alkene in favor of an ion-pairing interaction, we synthesized [(C₆H₅)₂CH₃NH][MeB(C₆F₅)₃] (**13**). Protonation of zirconacycle **7** with **13** gave two isomers of Cp*₂Zr[η¹,η²-CH₂CH(CH₃)CH₂CH=CH₂][MeB(C₆F₅)₃] (**14a** and **14b**). The ¹³C NMR chemical shift of the methyl group attached to boron was 10 ppm, characteristic of the free anion, with no interaction between the methyl group and the zirconium center. All other aspects of the NMR data are similar to those of the related B(C₆F₅)₄ ion pairs **8a** and **8b**. The barriers associated with alkene decomplexation and inversion were found to be unaffected by the change in counteranion. The binding of the chelated alkene in preference to the methylborate anion for our Cp*₂Zr systems contrasts with a preference for Zr–CH₃B ion-pairing over alkene complexation in the sterically less crowded Cp₂Zr system, which was predicted on the basis of DFT calculations.²¹

Discussion

Our earlier direct observation of d⁰ yttrium–alkyl–alkene chelates established the viability of d⁰ metal–alkyl–alkene complexes, which have been proposed as intermediates in metallocene-catalyzed alkene polymerizations. The current observations of cationic d⁰ zirconium–alkyl–alkene chelates are more closely related to catalytic systems. For the yttrium–alkyl–alkene chelates, alkene coordination resulted in shifts of the secondary vinyl ¹H and ¹³C NMR chemical shifts to higher frequency, which were attributed to polarization

of the alkene π-bond. For the cationic and therefore more electrophilic zirconium center, these high-frequency shifts were of greater magnitude, implying greater polarization of the alkene π-bond. In agreement with the hypothesis that alkenes should bind tighter to a more electron-deficient cationic zirconium center, 3 kcal mol^{−1} higher kinetic barriers for alkene dissociation were observed for the zirconium chelates compared with neutral yttrium chelates. Thermodynamic alkene binding energies to zirconium are expected to be greater than to yttrium. We have determined thermodynamic binding energies for alkene complexation in yttrium chelates by observing an equilibrium between bound and free alkene. We are searching for similar zirconium systems that will permit determination of alkene binding equilibrium constants. If successful, this will allow direct comparison of alkene binding energies in related zirconium and yttrium systems.

The barrier for site epimerization at zirconium (14.4 kcal mol^{−1}) was also found to be higher than in the corresponding yttrium complexes (9.6 kcal mol^{−1}). This can be partially attributed to alkene dissociation being the first step in this process, but the difference between the barriers for alkene dissociation and inversion is also greater for the zirconium (3.2 kcal mol^{−1}) complexes than the yttrium analogues (2.0 kcal mol^{−1}). This implies that the second step in site epimerization, inversion of stereochemistry at the zirconium center, also has a higher barrier than its yttrium relative (Figure 1). The barrier for site epimerization may arise from several different sources: (1) there may be an intrinsic barrier to inversion;²² (2) inversion may require the loss of a stabilizing agostic interaction;²³ (3) rotation about the M–CH₂ bond may be inhibited by steric repulsion between the alkyl chain and the Cp* ligands; and in the case of cationic zirconium, (4) inversion may require the loss of stabilizing interactions with solvent or tight ion-pairs.

(22) DFT and ab initio calculations predict a planar structure for methyl complexes of d⁰ metallocenes such as Cp₂ScCH₃. For ethyl and propylmetallocene complexes, the d⁰ metal center is predicted to adopt a pyramidal geometry in order to accommodate an energetically favorable β-CH agostic interaction. (a) Ziegler, T.; Folga, E.; Berces, A. *J. Am. Chem. Soc.* **1993**, *115*, 636. (b) Woo, T. K.; Fan, L.; Ziegler, T. *Organometallics* **1994**, *13*, 2252. (c) Yoshida, T.; Koga, N.; Morokuma, K. *Organometallics* **1995**, *14*, 746. (d) Weiss, H.; Ehrig, M.; Ahlrichs, R. *J. Am. Chem. Soc.* **1994**, *116*, 4919. (e) Kawamura-Kuribayashi, H.; Koga, N.; Morokuma, K. *J. Am. Chem. Soc.* **1992**, *114*, 8687.

(23) (a) Brookhart, M.; Green, M. L. H. *J. Organomet. Chem.* **1983**, *250*, 395. (b) Brookhart, M.; Green, M. L. H.; Wong, L. *Prog. Inorg. Chem.* **1988**, *36*, 1. (c) Grubbs, R. H.; Coates, G. W. *Acc. Chem. Res.* **1996**, *29*, 85.

(19) An attempt to use a nonchlorinated solvent, toluene-*d*₈, was unsuccessful. We believe that **8a** and **8b** form, but are insoluble in toluene at low temperature, where only **11** is observed by NMR.

(20) Yang, X.; Stern, C. L.; Marks, T. J. *J. Am. Chem. Soc.* **1994**, *116*, 10015.

(21) Chan, M. S. W.; Vanka, K.; Pye, C. C.; Ziegler, T. *Organometallics* **1999**, *18*, 4624.

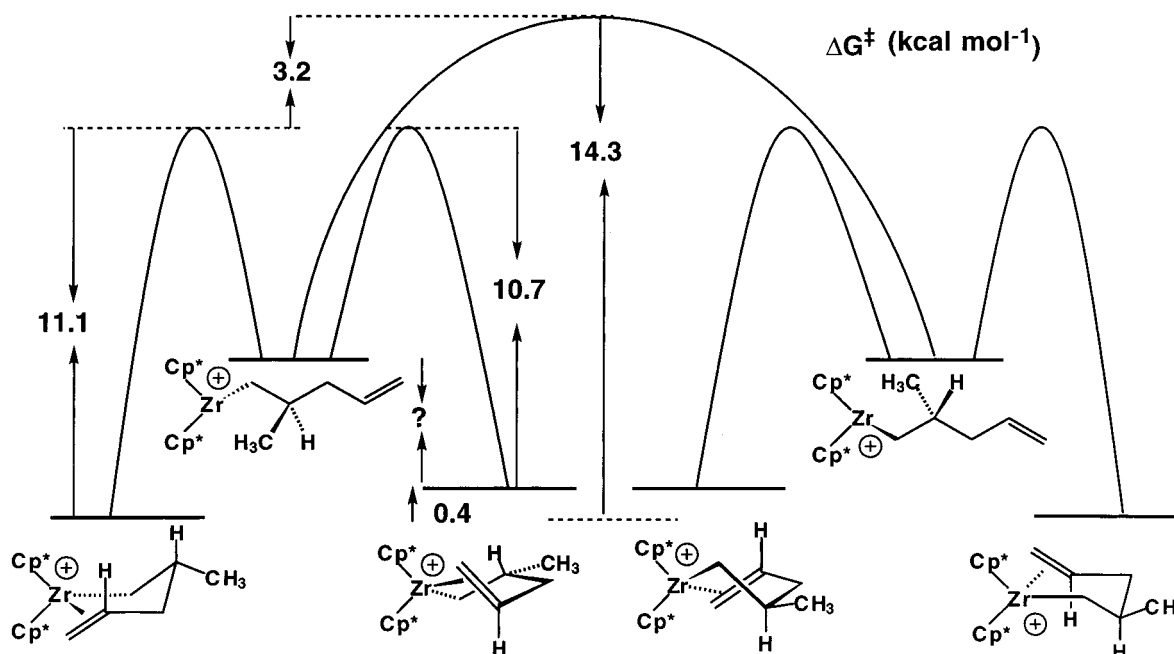
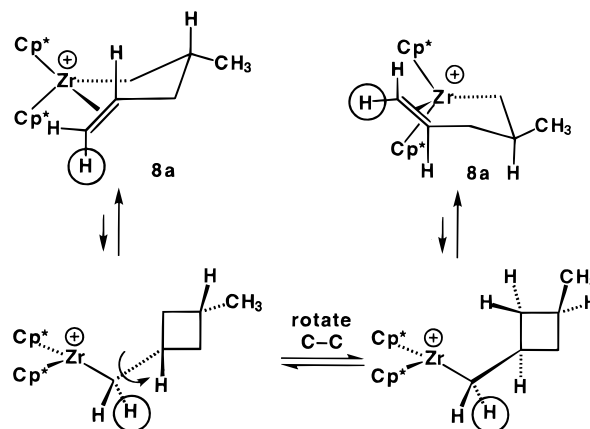


Figure 1. Free energy diagram for the barrier to alkene dissociation and site epimerization for $[\text{Cp}^*_2\text{ZrCH}_2\text{CH}(\text{CH}_3)\text{CH}_2\text{-CH=CH}_2][\text{B}(\text{C}_6\text{F}_5)_4]$ (**8a** and **8b**).

C_5 -symmetric metallocene catalysts produce highly syndiotactic polypropylene by a proposed mechanism in which stereospecific propene insertion is much more rapid than site epimerization (Scheme 2). Detailed understanding of syndiotactic polymerizations requires knowledge of the relative rates of alkene insertion and site epimerization. We have now determined that the barrier for site epimerization in our zirconium complexes is $14.4 \text{ kcal mol}^{-1}$. In future studies, we will attempt to measure the barrier for insertion of propene into a related cationic zirconium alkyl complex so that a quantitative comparison of the relative rates can be made.²⁴

To understand ligand control of stereochemistry in metallocene-catalyzed polymerizations, it is important to know whether stereochemistry is controlled by irreversible alkene coordination or by rate-determining alkyl migration to a reversibly bound alkene. In earlier studies of yttrium complexes, we used isotopic scrambling of $\text{Cp}^*_2\text{Y}(\eta^1, \eta^2\text{-CD}_2\text{CH}_2\text{CH}_2\text{CH=CD}_2)$ to determine the rate of reversible alkene insertion to give a strained cyclobutylmethyl yttrium intermediate. The barrier for this process was 10^8 times slower than alkene dissociation. We would like to know the related relative rates for the zirconium complexes reported here. In **8**, intramolecular insertion processes interchange the environments of the terminal vinyl hydrogens (Scheme 9). However, intramolecular alkene insertion was too slow to give rise to line broadening of the terminal vinyl ^1H NMR resonances. Saturation transfer experiments, which are capable of measuring slower rates than coalescence techniques, showed no evidence for interconversion of the terminal vinyl proton resonances at -10°C . This implies an insertion rate of less than 0.35 s^{-1} . At this point, we are only able to estimate that alkene decom-

Scheme 9



plexation is at least 10^4 faster than reversible alkene insertion to give a strained cyclobutylmethyl zirconium intermediate.

Alkene binding to the d^0 metal center is fairly weak as a result of the inability of the metal to back-donate electron density into the π^* orbitals of the alkene. As a result, many σ donors can compete with the alkene for binding to the metal center. We have found that THF, dimethylaniline, tributylamine, and diisopropyl(ethyl)amine are all better donors to the electrophilic zirconium center than the alkene chelate. In contrast, diphenyl(methyl)amine, a more sterically hindered and less Lewis basic amine, did not displace the alkene chelate. For future studies of the thermodynamics of alkene binding, we are seeking a Lewis base that binds competitively with the alkene.

Experimental Section

$[(\text{C}_6\text{H}_5)_2\text{CH}_3\text{NH}][\text{B}(\text{C}_6\text{F}_5)_4]$. A solution of $[(\text{C}_6\text{H}_5)_2\text{CH}_3\text{NH}]\text{-Cl}$ (2.56 g, 11.7 mmol) in 70 mL of CH_2Cl_2 was added via cannula to a solution of $\text{Li}[\text{B}(\text{C}_6\text{F}_5)_4]$ (11.8 g, 17.0 mmol) in 50 mL of CH_2Cl_2 . The resulting white slurry was stirred for 3 h,

(24) For a related yttrium system, we have measured the relative barriers of site epimerization and alkene insertion. Casey, C. P.; Lee, T.-Y.; Carpenetti, D. W., II. Manuscript in preparation.

filtered, and washed with CH_2Cl_2 . Solvent was evaporated from the combined filtrate under vacuum. The resulting solid was dissolved in a minimal amount of CH_2Cl_2 (50 mL), and hexane was added in small increments to give a light gray precipitate, which was isolated by filtration and dried under vacuum at 100 °C overnight to give $[(\text{C}_6\text{H}_5)_2\text{CH}_3\text{NH}][\text{B}(\text{C}_6\text{F}_5)_4]$ (8.0 g, 85%). ^1H NMR (500 MHz, CD_2Cl_2): δ 3.84 (s, 6H, CH_3), 7.41 (m, 4H, Ph), 7.65 (m, 6H, Ph), 8.61 (br s, 1H, NH).

$\text{Cp}^*\text{Zr}[\text{CH}_2\text{CH}(\text{CH}_2\text{CH}=\text{CH}_2)\text{CH}_2]$ (7) was prepared as reported by Stryker.¹² ^1H NMR (500 MHz, CD_2Cl_2): δ -0.23 (m, ZrCH_2CH), 0.69 (dd, J = 11.6, 10.6 Hz, ZrCHH), 1.11 (dd, J = 11.6, 9.2 Hz, ZrCHH), 1.66, 1.80 (s, C_5Me_5 's), 2.41 (tm, J = 7.0 Hz $\text{CH}_2\text{CH}=\text{CH}_2$), 5.14 (ddt, J = 10.1, 2.5, 1.2 Hz, $\text{CH}=\text{CHH}$), 5.25 (ddt, J = 17.1, 2.5, 1.2 Hz, $\text{CH}=\text{CHH}$), 6.29 (ddt, J = 17.1, 10.1, 7.0 Hz, $\text{CH}=\text{CH}_2$). ^{13}C NMR (gated decoupled, 126 MHz, CD_2Cl_2): δ 11.0 (q, J = 125 Hz, C_5Me_5), 12.0 (q, J = 125 Hz, C_5Me_5), 14.4 (br d, J = 127 Hz ZrCH_2CH), 44.5 (t, J = 127 Hz, $\text{CH}_2\text{CH}=\text{CH}_2$), 60.3 (t, J = 129 Hz, ZrCH_2), 113.9 (t, J = 153 Hz, $\text{CH}=\text{CH}_2$), 115.5 (C_5Me_5), 116.2 (C_5Me_5), 141.2 (d, J = 149 Hz, $\text{CH}=\text{CH}_2$).

Reaction of $\text{Cp}^*\text{Zr}[\text{CH}_2\text{CH}(\text{CH}_2\text{CH}=\text{CH}_2)\text{CH}_2]$ (7) with $\text{B}(\text{C}_6\text{F}_5)_3$. CD_2Cl_2 (0.5 mL) was condensed into a resealable NMR tube containing 7 (20 mg, 0.045 mmol) and $\text{B}(\text{C}_6\text{F}_5)_3$ (23.0 mg, 0.045 mmol) at -78 °C. The tube was shaken briefly at -78 °C to give a bright orange solution and was inserted into the precooled probe of the NMR spectrometer. The NMR spectra showed a 1.8:1 mixture of isomers of $\text{Cp}^*\text{Zr}[\eta^1, \eta^2\text{-CH}_2\text{-CH}(\text{CH}_2\text{B}(\text{C}_6\text{F}_5)_3)\text{CH}_2\text{CH}=\text{CH}_2]$ (**2a** and **2b**) whose NMR spectra at various temperatures are given below.

$\text{Cp}^*\text{Zr}[\eta^1, \eta^2\text{-CH}_2\text{CH}(\text{CH}_2\text{B}(\text{C}_6\text{F}_5)_3)\text{CH}_2\text{CH}=\text{CH}_2]$ (2a**, major isomer).** ^1H NMR (500 MHz, CD_2Cl_2 , -82 °C): δ -0.84 (br d, ZrCH_2CH), 0.85 (br d, J = 7 Hz, ZrCH_2), 1.96 (br s, C_5Me_5), 1.98 (br s, C_5Me_5), 2.44 (br d, J_{cis} = 10.1 Hz, $=\text{CHH}$), 5.85 (br d, J_{trans} = 17.1 Hz, $=\text{CHH}$), 7.92 (m, J = 17.1, 10.1 Hz, $\text{CH}=\text{CH}_2$); resonances for CH_2B and $\text{CH}_2\text{CH}=\text{CH}_2$ were observed by TOCSY1D NMR at 2.18 (1H), 2.04 (1H), and 1.72 (2H) but were not assigned. ^{13}C NMR (gated decoupled, 126 MHz, CD_2Cl_2 , -82 °C): δ 11.3 (q, J = 127 Hz, C_5Me_5), 11.4 (q, J = 127 Hz, C_5Me_5), 26.9 (t, J = 122 Hz, BCH_2), 27.7 (d, J = 127 Hz, ZrCH_2CH), 43.0 (t, J = 135 Hz, $\text{CH}_2\text{CH}=\text{CH}_2$), 75.7 (t, J = 119 Hz, ZrCH_2), 114.9 (t, J = 154 Hz, $\text{CH}=\text{CH}_2$), 124.3 (s, C_5Me_5), 124.4 (s, C_5Me_5), 163.6 (d, J = 153 Hz, $\text{CH}=\text{CH}_2$), 118.8 (br s, BC_{ipso}), 136.1 (d, J_{CF} = 247 Hz, CF), 138.6 (d, J_{CF} = 262, CF), 146.9 (d, J_{CF} = 238 Hz, CF).

$\text{Cp}^*\text{Zr}[\eta^1, \eta^2\text{-CH}_2\text{CH}(\text{CH}_2\text{B}(\text{C}_6\text{F}_5)_3)\text{CH}_2\text{CH}=\text{CH}_2]$ (2b**, minor isomer).** ^1H NMR (500 MHz, CD_2Cl_2 , -82 °C): δ -1.13 (br d, ZrCH_2CH), 0.83 (br d, J = 7 Hz, ZrCH_2), 1.94 (br s, C_5Me_5), 1.96 (br s, C_5Me_5), 2.47 (br d, J_{cis} = 12.5 Hz, $=\text{CHH}$), 5.73 (br d, J_{trans} = 17.8 Hz, $=\text{CHH}$), 7.54 (m, J = 17.8, 12.5 Hz, $\text{CH}=\text{CH}_2$); resonances for BCH_2 and $\text{CH}_2\text{CH}=\text{CH}_2$ were observed by TOCSY1D NMR at 2.45 (1H), 2.16 (1H), and 1.68 (2H) but were not assigned. ^{13}C NMR (gated decoupled, 126 MHz, CD_2Cl_2 , -82 °C): δ 11.6 (q, J = 127 Hz, C_5Me_5), 12.0 (q, J = 127 Hz, C_5Me_5), 30.0 (t, J = 135 Hz, CH_2B), 31.7 (d, J = 124 Hz, ZrCH_2CH), 38.7 (t, J = 135 Hz, $\text{CH}_2\text{CH}=\text{CH}_2$), 73.2 (t, J = 119 Hz, ZrCH_2), 114.2 (t, J = 158 Hz, $\text{CH}=\text{CH}_2$), 124.7 (s, C_5Me_5), 125.1 (s, C_5Me_5), 166.7 (d, J = 151 Hz, $\text{CH}=\text{CH}_2$), 118.8 (br s, BC_{ipso}), 136.1 (d, J_{CF} = 247 Hz, CF), 137.6 (d, J_{CF} = 262, CF), 146.9 (d, J_{CF} = 238 Hz, CF).

$\text{Cp}^*\text{Zr}[\eta^1, \eta^2\text{-CH}_2\text{CH}(\text{CH}_2\text{B}(\text{C}_6\text{F}_5)_3)\text{CH}_2\text{CH}=\text{CH}_2]$ (2**, rapidly equilibrating mixture of **2a** and **2b** at -32 °C).** ^1H NMR (500 MHz, CD_2Cl_2 , -32 °C): δ 7.79 (m, J = 17.3, 10.0 Hz, $\text{CH}=\text{CH}_2$), 5.82 (br d, J = 17.3, $\text{CH}=\text{CHH}$), 2.47 (br d, J = 10.0 Hz, $\text{CH}=\text{CHH}$), 2.03 (s, C_5Me_5), 2.01 (s, C_5Me_5), 0.85 (d, J = 7 Hz, ZrCH_2), -0.86 (br d, J = 10.6 Hz, ZrCH_2CH). Resonances corresponding to $\text{CH}_2\text{CH}=\text{CH}_2$ and BCH_2 were observed at δ 2.33, 2.11, and 1.74 but were not assigned.

Reaction of $\text{Cp}^*\text{Zr}[\text{CH}_2\text{CH}(\text{CH}_2\text{CH}=\text{CH}_2)\text{CH}_2]$ (7) with $[(\text{C}_6\text{H}_5)_2(\text{CH}_3)\text{NH}][\text{B}(\text{C}_6\text{F}_5)_4]$. CD_2Cl_2 (0.5 mL) was condensed into a resealable NMR tube containing 7 (20 mg, 0.045 mmol) and $[(\text{C}_6\text{H}_5)_2(\text{CH}_3)\text{NH}][\text{B}(\text{C}_6\text{F}_5)_4]$ (39.0 mg, 0.045 mmol) at -78

°C. The tube was shaken briefly at -78 °C to give a bright orange solution and was inserted into the precooled probe of the NMR spectrometer. The NMR spectra showed a 2.2:1 mixture of isomers of $\text{Cp}^*\text{Zr}[\eta^1, \eta^2\text{-CH}_2\text{CH}(\text{CH}_3)\text{CH}_2\text{CH}=\text{CH}_2][\text{B}(\text{C}_6\text{F}_5)_4]$ (**8a** and **8b**) and $(\text{C}_6\text{H}_5)_2\text{CH}_3\text{N}$ (**11**), whose NMR spectra at various temperatures are given below. More dilute CD_2Cl_2 solutions and a solution in $\text{C}_6\text{D}_5\text{Cl}$ were also prepared.

$\text{Cp}^*\text{Zr}[\eta^1, \eta^2\text{-CH}_2\text{CH}(\text{CH}_3)\text{CH}_2\text{CH}=\text{CH}_2][\text{B}(\text{C}_6\text{F}_5)_4]$ (8a**, major isomer).** ^1H NMR (500 MHz, CD_2Cl_2 , -78 °C): δ -0.83 (br d, ZrCH_2CH), 0.85 (br d, J = 7 Hz, ZrCH_2), 1.96 (br s, C_5Me_5), 1.98 (br s, C_5Me_5), 2.44 (br d, J_{cis} = 10.1 Hz, $=\text{CHH}$), 5.43 (br d, J_{trans} = 17.1 Hz, $=\text{CHH}$), 7.89 (m, J = 17.1, 10.1 Hz, $\text{CH}=\text{CH}_2$); resonances for CH_3 and $\text{CH}_2\text{CH}=\text{CH}_2$ were observed by TOCSY1D NMR at 1.70 and 2.20 but were not assigned. ^{13}C NMR (gated decoupled, 126 MHz, CD_2Cl_2 , -78 °C): δ 10.7 (q, J = 127 Hz, C_5Me_5), 10.8 (q, J = 127 Hz, C_5Me_5), 21.3 (q, J = 122 Hz, CH_3), 26.4 (t, J = 123 Hz, $\text{CH}_2\text{CH}=\text{CH}_2$), 31.2 (d, J = 120 Hz, ZrCH_2CH), 75.1 (t, J = 119 Hz, ZrCH_2), 113.7 (t, J = 155 Hz, $\text{CH}=\text{CH}_2$), 123.8 (s, C_5Me_5), 123.9 (s, C_5Me_5), 163.0 (d, J = 153 Hz, $\text{CH}=\text{CH}_2$), 121.0 (br s, BC_{ipso}), 135.1 (d, J_{CF} = 238 Hz, CF), 137.0 (d, J_{CF} = 243, CF), 146.8 (d, J_{CF} = 239 Hz, CF). ^{19}F NMR (416.5 MHz, CD_2Cl_2 , -78 °C): δ -135.9 (s, 8F), -166.2 (t, J_{FF} = 19.7 Hz, 4F), -170.2 (s, 8F).

$\text{Cp}^*\text{Zr}[\eta^1, \eta^2\text{-CH}_2\text{CH}(\text{CH}_3)\text{CH}_2\text{CH}=\text{CH}_2][\text{B}(\text{C}_6\text{F}_5)_4]$ (8b**, minor isomer).** ^1H NMR (500 MHz, CD_2Cl_2 , -78 °C): δ -1.12 (br d, ZrCH_2CH), 0.83 (br d, J = 7 Hz, ZrCH_2), 1.96 (br s, C_5Me_5), 1.98 (br s, C_5Me_5), 2.18 (br d, J_{cis} = 12.5 Hz, $=\text{CHH}$), 5.71 (br d, J_{trans} = 17.8 Hz, $=\text{CHH}$), 7.49 (m, J = 17.8, 12.5 Hz, $\text{CH}=\text{CH}_2$); resonances for CH_3 and $\text{CH}_2\text{CH}=\text{CH}_2$ were observed by TOCSY1D NMR at 2.25 and 1.85 but were not assigned. ^{13}C NMR (gated decoupled, 126 MHz, CD_2Cl_2 , -78 °C): δ 11.0 (q, J = 127 Hz, C_5Me_5), 11.6 (q, J = 127 Hz, C_5Me_5), 22.0 (q, J = 128 Hz, CH_3), 26.1 (t, J = 122 Hz, $\text{CH}_2\text{CH}=\text{CH}_2$), 29.5 (d, J = 120 Hz, ZrCH_2CH), 72.6 (t, J = 129 Hz, ZrCH_2), 110.6 (t, J = 157 Hz, $\text{CH}=\text{CH}_2$), 124.2 (s, C_5Me_5), 124.6 (s, C_5Me_5), 166.1 (d, J = 152 Hz, $\text{CH}=\text{CH}_2$), 121.0 (br s, BC_{ipso}), 135.1 (d, J_{CF} = 238 Hz, CF), 137.0 (d, J_{CF} = 243, CF), 146.8 (d, J_{CF} = 239 Hz, CF). ^{19}F NMR (416.5 MHz, CD_2Cl_2 , -78 °C): δ -135.9 (s, 8F), -166.2 (t, J_{FF} = 19.7 Hz, 4F), -170.2 (s, 8F).

$(\text{C}_6\text{H}_5)_2\text{NCH}_3$ (11**).** ^1H NMR (500 MHz, CD_2Cl_2 , -78 °C): δ 3.18 (s, NCH_3), 7.09 (m, 4H, Ph), 7.33 (m, 6H, Ph). ^{13}C NMR (gated decoupled, 126 MHz, CD_2Cl_2 , -78 °C): δ 41.5 (q, J = 139 Hz, NCH_3), 119.4 (br, m-Ph), 123.1 (br, p-Ph), 128.9 (dd, J = 159, 7 Hz, o-Ph), 145.3 (s, ipso-Ph).

$\text{Cp}^*\text{Zr}[\eta^1, \eta^2\text{-CH}_2\text{CH}(\text{CH}_3)\text{CH}_2\text{CH}=\text{CH}_2]$ (rapidly equilibrating mixture of **8a and **8b** at -38 °C).** ^1H NMR (500 MHz, CD_2Cl_2 , -38 °C): δ -0.85 (br, ZrCH_2CH), 0.84 (d, J = 7 Hz, ZrCH_2), 2.00 (s, C_5Me_5), 2.02 (s, C_5Me_5), 2.40 (br d, J = 10.0 Hz, $\text{CH}=\text{CHH}$), 5.82 (br d, J = 17.3, $\text{CH}=\text{CHH}$), 7.84 (br, $\text{CH}=\text{CH}_2$). Resonances corresponding to $\text{CH}_2\text{CH}=\text{CH}_2$ and CH_3 were observed at δ 2.33 and 1.84 but were not assigned. ^1H NMR (500 MHz, $\text{C}_6\text{D}_5\text{Cl}$, -38 °C): δ -0.92 (br, ZrCH_2CH), 1.08 (d, J = 7 Hz, ZrCH_2), 1.80 (s, C_5Me_5), 1.82 (s, C_5Me_5), 2.63 (br d, J = 10.0 Hz, $\text{CH}=\text{CHH}$), 5.27 (br d, J = 17.3, $\text{CH}=\text{CHH}$), 7.56 (br, $\text{CH}=\text{CH}_2$). Resonances corresponding to $\text{CH}_2\text{CH}=\text{CH}_2$ and CH_3 were observed at δ 2.24 and 1.92 but were not assigned.

$\text{Cp}^*\text{Zr}[\eta^1, \eta^2\text{-CH}_2\text{CH}(\text{CH}_3)\text{CH}_2\text{CH}=\text{CH}_2]$ (rapidly equilibrating mixture of **8a and **8b** at 2 °C).** ^1H NMR (500 MHz, CD_2Cl_2 , 2 °C): δ -0.85 (br, ZrCH_2CH), 0.84 (br, ZrCH_2), 2.05 (s, C_5Me_5), 2.46 (br, $\text{CH}=\text{CHH}$), 5.78 (br, $\text{CH}=\text{CHH}$), 7.79 (br, $\text{CH}=\text{CH}_2$). Resonances corresponding to $\text{CH}_2\text{CH}=\text{CH}_2$ and CH_3 were obscured by decomposition products and were not observed. ^1H NMR (500 MHz, $\text{C}_6\text{D}_5\text{Cl}$, 2 °C): δ -0.92 (br, ZrCH_2CH), 1.08 (br, ZrCH_2), 1.90 (s, C_5Me_5), 2.67 (br, $\text{CH}=\text{CHH}$), 5.20 (br, $\text{CH}=\text{CHH}$), 7.49 (br, $\text{CH}=\text{CH}_2$). Resonances corresponding to $\text{CH}_2\text{CH}=\text{CH}_2$ and CH_3 were obscured by decomposition products and were not observed.

$\{\text{Cp}^*\text{Zr}[\text{N}(\text{CH}_3)_2\text{C}_6\text{H}_5][\text{CH}_2\text{CH}(\text{CH}_3)\text{CH}_2\text{CH}=\text{CH}_2][\text{B}(\text{C}_6\text{F}_5)_4]$ (10**).** CD_2Cl_2 (0.5 mL) was condensed into a

resealable NMR tube containing **7** (20 mg, 0.045 mmol) and $[\text{C}_6\text{H}_5(\text{CH}_3)_2\text{NH}][\text{B}(\text{C}_6\text{F}_5)_4]$ (36 mg, 0.045 mmol) at -78°C . The tube was shaken briefly at -78°C to give a yellow solution of **10**. ^1H NMR (500 MHz, CD_2Cl_2 , -78°C): δ 0.18 (br, ZrCH_2CH), 0.66 (br d, $J = 7$ Hz, $\text{ZrCH}_2\text{CHCH}_3$), 0.82 (br d, ZrCH_2), 1.86 (s, C_5Me_5), 2.16 (m, $\text{CH}_2\text{CH}=\text{CH}_2$), 3.65 (s, $\text{N}(\text{CH}_3)_2$), 4.82 (br d, $J_{\text{cis}} = 10.1$ Hz, $\text{CH}=\text{CHH}$), 4.84 (br d, $J_{\text{trans}} = 17.1$ Hz, $\text{CH}=\text{CHH}$), 5.70 (dd br t, $J = 17.1$, 10.1, $\text{CH}=\text{CH}_2$).

Acknowledgment. Financial support from the National Science Foundation (CHE-9972183) is gratefully acknowledged. Grants from the NSF (CHE-9629688) for the purchase of NMR spectrometers are acknowledged. We thank Dr. Charles Fry for helpful discussions.

Supporting Information Available: General experimental, preparations of $[\text{C}_6\text{H}_5(\text{CH}_3)_2\text{NH}][\text{B}(\text{C}_6\text{F}_5)_4]$, $[(\text{C}_6\text{H}_5)_2\text{CH}_3\text{NH}][\text{CH}_3\text{B}(\text{C}_6\text{F}_5)_3]$ (**13**), $[\text{C}_6\text{H}_5(\text{CH}_3)_3\text{N}][\text{MeB}(\text{C}_6\text{F}_5)_3]$, $[\text{C}_6\text{H}_5(\text{CH}_3)_3\text{N}][\text{B}(\text{C}_6\text{F}_5)_4]$, $\text{Cp}^*_2\text{Zr}(\text{THF})[\text{CH}_2\text{CH}(\text{CH}_2\text{B}^-(\text{C}_6\text{F}_5)_3)\text{CH}_2\text{CH}=\text{CH}_2]$ (**9**), $\text{Cp}^*_2\text{Zr}(\text{THF})[\text{CH}_2\text{CH}(\text{CH}_3)\text{CH}_2\text{CH}=\text{CH}_2][\text{B}(\text{C}_6\text{F}_5)_4]$ (**11**), $\{\text{Cp}^*_2\text{Zr}[\text{N}(\text{CH}_2\text{CH}_2\text{CH}_2\text{CH}_3)_3]\text{CH}_2\text{CH}(\text{CH}_3)\text{CH}_2\text{CH}=\text{CH}_2\}-[\text{B}(\text{C}_6\text{F}_5)_4]$, $\{\text{Cp}^*_2\text{Zr}[\text{N}(\text{CHMe}_2)_2\text{Et}]\text{CH}_2\text{CH}(\text{CH}_3)\text{CH}_2\text{CH}=\text{CH}_2\}-[\text{B}(\text{C}_6\text{F}_5)_4]$, reaction of $\text{Cp}^*_2\text{Zr}[\text{CH}_2\text{CH}(\text{CH}_2\text{CH}=\text{CH}_2)\text{CH}_2]$ (**7**) with $[(\text{C}_6\text{H}_5)_2(\text{CH}_3)\text{NH}][\text{MeB}(\text{C}_6\text{F}_5)_3]$ (**13**), and temperature-dependent ^1H NMR spectra of **8a** and **8b**. This material is available free of charge via the Internet at <http://pubs.acs.org>.

OM9908940